Available online at www.sciencedirect.com
ScienceDirect
Polymer 48 (2007) 7645–7652
polymer
www.elsevier.com/locate/polymer

Studies on flow behaviors of polymer melts in nanochannels by wetting actions

Kai-Leung Yung [a], Jie Kong [a,b,*], Yan Xu [a]

[a] Department of Industrial and Systems Engineering, The Hong Kong Polytechnic University, Hung Hom, Kowloon, Hong Kong, China
[b] Department of Applied Chemistry, School of Science, Northwestern Polytechnical University, Xi'an 710072, PR China

Received 12 August 2007; received in revised form 18 October 2007; accepted 4 November 2007
Available online 12 November 2007

Abstract

The flow behavior of polymer melts in nanochannels by wetting actions was investigated by statistical analyses of generated polymer nanofibers' length in nanochannels of nanoporous alumina template using Scanning Electron Microscopy. The polyethylene nanofibers with high aspect ratio are formed after the infiltration of melts into the alumina nanochannels by wetting actions. The wetting of polyethylene melts in nanochannels is a rapid process due to the high surface free energy of inner walls and wetting driven force. Wetting and flow rate of polymer melts in nanochannels are mainly dependent on the wetting temperature, the size of nanochannels and surface properties of nanochannels adjusted by octadecyltrimethoxysilane self-assembled monolayers. High surface free energy and solid–liquid interaction between melts and surface lead to noticeable flow of polymer melts in nanochannels at the wetting stage.
© 2007 Elsevier Ltd. All rights reserved.

Keywords: Nanochannel; Flow; Wetting

1. Introduction

Micro-/nanoelectromechanical systems (M/NEMS), micro-total analytical system (μ-TAS), and ''lab-on-a-chip'' are of tremendous interest due to their potential applications in communications, electro-mechanism, energy, biology and medical fields [1–3]. Recently the polymer micro-/nano-biosensors and biochips have attracted more and more attentions for their promoting efficiency, disposability and biocompatibility [4–6]. Lots of micro-/nano-processing approaches, such as capillary lithography, nanoimprint lithography, microstereolithography, electro-spinning, and micro-/nano-injection, casting or extrusion [7–14] have been developed to fabricate these micro-/nano-polymer devices and systems. For the lithography or micro-/nano-injection, a key factor is the favorable flow of polymer melts in nanochannels, nanopores or nanolayers. Compared with the hydrodynamic fluidics of simple liquid in micro-, meson- or macro-channel, the flow behavior of polymer melts in nanochannels is more strongly determined by the nanoscale effect and surface interaction, such as capillary effect, surface energy, wettability property and roughness of inner walls of nanochannels. Even for the simple liquid, the classical macroscopic capillarity theory often fails to describe its flow behavior in a nanochannel with water–hydrophobic interface [15], so the flow behavior of polymer melts in nanochannels is not well defined up to now.

Due to the difficulty in achieving a favorable flow of liquid in nanochannels, many researchers focused on the simulations of nanoflow of simple liquid in nanochannels mainly using molecular dynamics (MD) and Monte Carlo (MC) methods [16–20]. The boundary condition, slip and viscosity of simple molecule or liquid in nanochannels are usually analyzed to study the effects of channel characteristics such as roughness and wettability. Galea and Attard [16] found that the fluid–solid slip of simple LJ liquid occurred for both smooth and rough surfaces and slip length exhibited nonmonotonic behavior as the solid structure was varied from smooth to rough.

* Corresponding author. Department of ISE, The H.K. Polytechnic University, Hung Hom, Kowloon, Hong Kong, China. Tel.: +852 3400 3241; fax: +852 3400 3244.
E-mail address: mfkongjie@hotmail.com (J. Kong).

0032-3861/$ - see front matter © 2007 Elsevier Ltd. All rights reserved.
doi:10.1016/j.polymer.2007.11.013

Bonaccurso et al. [17] presented that the degree of hydrodynamic boundary slip of a newtonian fluid was increased with the increase of surface roughness in complete wetting system. In our previous works [21–23], the effects of roughness, including period and amplitude of serrations of nanochannels, on the flowability of liquid crystal polymers (LCP) were analyzed using novel GB-spring-bead model. These MD simulation results reveal that the roughness amplitude, slippage, shear rates and surface energy of inner wall all have profound influences on the fluid viscosity and fluid–solid boundary conditions of LCP in nanochannels. So far, it has been accepted in theory that the nature of the shear rate, liquid–solid interface, in particular surface wettability and roughness play important roles on the slip behavior of simple liquid on interface or in micro-/nano-channel [24].

For the verification of simulation results on boundary condition and slip of liquid on interface, some characterization techniques have been developed, which includes fluorescent recovery after photo-bleaching [25], using tracers to follow liquid flow [26], surface forces apparatus [27], and small angle X-ray scattering [28], etc. And other experimental methods, such as inducing glycerin and ionic salts flow through a single nanopipe driven by the pressure difference between two liquid drops with different shapes and sizes [29] and pressure driven flow of classical fluids through lithographically produced channels [30] were also presented. However, the realization and visual experimental characterization of flow of polymer melts with high viscosity and elasticity in nanochannels are very difficult, and few features are definite though it is very important for achieving polymer-based micro-/nano-devices *via* lithography or nano-injection/casting. The main reason is that the surface effects between inner walls and melts become the key factors to determine the polymer melts' permeation and flow behaviors through nanochannels. To assure the stable flow of melts with high viscosity and elasticity, the driven pressure is often out of the acceptance of laboratory and engineering when the channel's diameter is decreased to nanoscale. To achieve the flow of polymer melts in nanochannels, from our viewpoint, the wetting phenomenon of liquid on a high-energy surface should be adequately noticed [31,32]. In fact, the well comprehension of wetting of polymer melts on a high-energy surface of metal oxide or silicon has promoted the fabrication of polymer one-dimensional nanostructures, such as nanopillars, nanofibers and nanotubes [33–37] since Steinhart et al. [38] for the first time presented the preparation of polymer nanotubes using nanoporous template wetting. If the nanochannels in lithography or nano-injection are prepared using materials with high surface energy, the polymer melts with low surface energy can wet and permeate into them favorably. So in an adequate time scale, the flow of polymer melts in nanochannels can be conveniently achieved and visually observed.

In this paper, for the first time, the displacement and rate of polymer melts in nanochannels of nanoporous anodic alumina template by wetting actions are studied by a facile statistical analyses strategy, i.e. determining the length of the generated model polymer nanofibers wetted in nanochannels at different times using Scanning Electron Microscopy. The influences of wetting temperature, nanochannels size, and nanochannel surface properties modified by self-assembled monolayers on the nanoflow behaviors of polyethylene in nanochannels are discussed. The results will provide fundamental guidelines for the preparation of polymer-based nanomaterials and nano-devices using lithography and potential nano-injection/casting nanotechnologies.

2. Experiments

2.1. Materials

Aluminum foils (purity: 99.9995%, thickness: 0.13 mm), $H_2C_2O_4$, phosphocromic acid, perchloric acid, Cr_2O_3, $CuCl_2$, NaOH, ethanol, acetone and deionized water were purchased from Alfa Aesar China Co. Ltd. Octadecyltrimethoxysilane, chloroform and hexane were obtained from Hong Kong Advanced Technology and Industrial Co., Ltd. The high-density polyethylene with density of 0.945 g/cm^3 and melting index of 13.0 g/10 min was obtained from Qilu Petroleum and Chemical Co. of China. The number-average molecular weight is 11,000 g/mol and the polydispersity index is 17.7, determined using PL220 high-temperature SEC.

2.2. Preparation of nanoporous anodic alumina templates

Nanoporous anodic alumina template (PAA) was prepared by two-step anodic oxidation. The aluminum foil was annealed at 450 °C for 5 h to perfect its crystalline structures. To obtain the polished surface of aluminum foil, electropolishing was conducted with a cleaned stainless steel as cathode at ambient temperature. The electrolyte was composed of perchloric acid and ethanol with a volume ratio of 1:4. Aluminum foil and the stainless steel were placed facing each other in the beaker with violent stirring of electrolyte solution. A DC voltage of 40 V was applied on the electrodes for 10 s during the electropolishing process.

After electropolishing, the standard two-step anodization was conducted to fabricate the PAA template. One surface of aluminum foil was firstly coated with nail polish (Maybelline Colorama). Anodization was performed at DC 40 V and 25 °C in a 0.5 M oxalic acid solution. The first anodization lasted for 0.5 h, and the second one lasted 2 h. During the interval of two stages, the partly oxidized foil was put into a mixed solution of 6% H_3PO_4 and 2% CrO_3 at 60 °C under ultrasonic treatment for 20 min to remove the aluminum oxide generated on the aluminum foil surface. After the second anodization, the sample was washed with deionized water. The remaining aluminum substrate was removed by immersing the as-prepared template in a $CuCl_2$-based solution (40 mL of HCl (38%) + 100 mL of H_2O + 3.4 g of $CuCl_2 \cdot 2H_2O$) at 25 °C for about 2 h. Then the bottom of the pores was subsequently opened by 0.1 M phosphoric acid at 35 °C. Before the removal of the aluminum substrate and enlarging pores, nail polish was coated on the top surface of

the PAA film, serving as a protective layer. At the end of process, the nail polish layer was peeled off using tweezers. The sample was then soaked in deionized water and ethanol for 15 min, resulting in the formation of a clean through-hole PAA template.

2.3. Surface modification of nanochannels of PAA templates

The PAA template was firstly treated using solvents with different polarity under ultrasonic treatment (ethanol, acetone, chloroform and hexane in sequence). Subsequently, octadecyltrimethoxysilane (OTMS) self-assembled monolayers were prepared on the alumina surface of PAA nanochannel to adjust their surface wettability properties. The PAA template was immersed into a solution of 5% (v/v) OTMS and 16 mM acetic acid in ethanol/water (95% v/v) for 60 min at room temperature followed by being cured at 150 °C for 2 h. After hydrolysis, condensation and subsequent curing at high temperature, the cross-linking reaction of OTMS was performed, and self-assembled monolayers on surface of nanochannels could be obtained.

As a comparison of surface properties, the static contact angle of *n*-hexadecane (non-polar, with similar molecular structure as polyethylene) on OTMS self-assembled monolayers modified alumina surface and native alumina surface was determined using a Rame-hart Model 250-F1 standard contact angle meters. The weight of polyethylene melts drop is about 5.0 mL and six parallel measurements were made for each sample.

2.4. Characterization of flow behaviors of polymer melts in PAA template

A facile strategy to study the flow behaviors was employed here. The displacement and rate of melts were deduced by statistical analyses of generated polymer nanofibers' length in nanochannels via Scanning Electron Microscopy. At first, polyethylene film with a thickness of about 300 μm was placed on the top of PAA template. Then, the polyethylene/template was assembled in a mould to ensure a good contact between the PE film and template and then put it into the hot oven, which had been heated to the set temperature. After the infiltration of melts for different times, the mould was taken out of the hot oven and cooled to ambient temperature. At last, the polyethylene nanofibers' arrays were released from the PAA template by removing the template using a NaOH solution and well rained by deionized water and ethanol. The nanofibers were characterized using Scanning Electron Microscopy (SEM, Leica Stereoscan 440) and Field-emission Scanning Electron Microscopy (FE-SEM, JEOL JSM-6335F). All samples were coated with 5 nm Au before measurements.

In addition, the released nanofibers were also characterized using Transmission Electron Microscopy (TEM, Philips CM120) at an accelerating voltage of 80 kV. Before the TEM observation, the nanostructures were sonicated in ethanol for 10 min and placed onto carbon-coated copper grids. The melting behavior of polyethylene was characterized using Differential Scanning Calorimeter (MDSC2910, Waters-TA Instruments) equipped with a refrigerated cooling system (RCS). The temperature was calibrated with indium. The furnace was purged with dry nitrogen at a flow rate of 50 mL/min. About 5.0 mg of sample was sealed in an aluminum pan, and the heating scanning was conducted from −20 °C to 180 °C at a scanning rate of 10 K/min.

3. Results and discussion

3.1. Establishment of characterization strategy for flow in nanochannels

For the investigation of flow behaviors of polymer melts in these through-hole nanochannels, the dynamic parameters such as driven force p, displacement l_t and rate dl_t/dt are considered as illustrated in Fig. 1. Due to the high surface energy of alumina, polymer melts with low surface energy can be wetting the surface in a partial or complete wetting regime and the wetting driven force p from high-energy surface can be described as the following *Laplace* equation [39]:

$$p = 2\gamma \cos \theta / R \tag{1}$$

where γ is surface tension of polymer melts on alumina surface, θ is contact angle, R is hydraulic radius and equal to half of radius of a nanochannel. In particular, the contact angle θ is determined by the solid–gas (γ_{SG}), solid–liquid (γ_{SL}), and liquid–gas (γ_{LG}) interfacial tensions as shown in Fig. 1.

The displacement l_t of melts into nanochannels at the time t and the rate dl_t/dt can be employed to visually describe the nanoflow behaviors. The small angle X-ray scattering [28] and fluorescence confocal microscope [40,41] have been

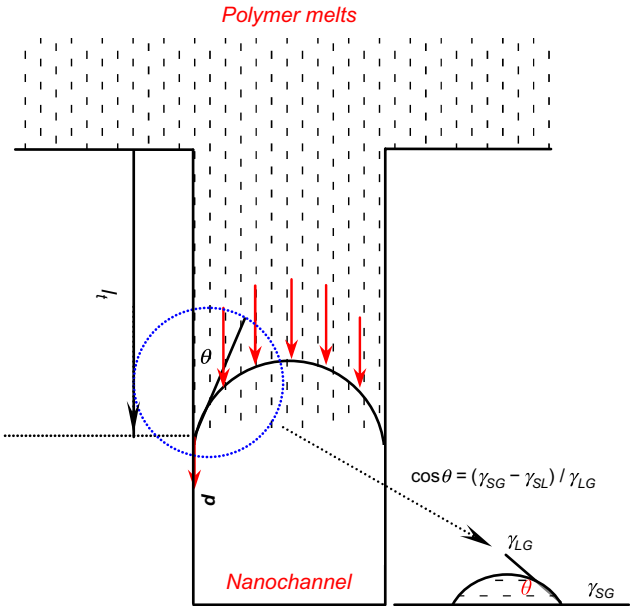

Fig. 1. Dynamic parameters of nanoflow of polymer melts in nanochannels, the p, l_t, θ and γ_{SG}, γ_{SL}, γ_{LG} are driven force, displacement, contact angle and solid–gas, solid–liquid, liquid–gas interfacial tensions, respectively.

used to study the diffusion of the sample liquid including methanol in silica nanotubes or alumina nanopores. However, considering the difficulty in fluorescence bleaching of the polymer melts with high viscosity and dynamic non-harmony between X-ray scatterings and the melts flow in nanochannels without shear actions [42–44], hereby, a facile statistical analysis strategy to study the nanoflow behaviors is employed. The displacement and rate of melts are deduced by statistical analyses of the generated polymer nanofibers' length in nanochannels at different wetting times.

The nanochannels of nanoporous alumina template were prepared by two-step anodic oxidation [45,46]. The SEM images in Fig. 2 indicate that self-organized, well-ordered, and parallel nanochannels have been obtained in PAA template. The diameter of monodispersed nanochannels presented here is around 60–80 nm and the length of nanochannels is 50 μm that is equal to the thickness of template as presented in Fig. 2C. At the wetting temperature far above the melting temperature (T_m), the polyethylene melts infiltrated into nanochannels of alumina template due to the wetting actions [47,48]. Polyethylene nanofibers with an average diameter of 80 nm and a length or height of 50 μm aligned in a direction nearly perpendicular to the remaining bulk substrate were obtained as presented in Fig. 3. The length or height of the generated nanofiber can represent the trace of polymer melts permeated into nanochannels before their condensation. After the removal of PAA template in NaOH solution, the length or height of nanofibers aligned on the remaining bulk film can be conveniently determined from their cross-section SEM image (Fig. 3C).

Since the length of the nanochannels (micrometer scale) is much smaller than the so-called capillary length κ^{-1} in millimeter scale ($\kappa^{-1} = \gamma^{0.5}/(\rho g)^{0.5}$, where ρ and g are the density of polymer melts and gravitational constant, respectively), gravitational influence on nanoflow of polymer melts can be negligible [48]. So the influences of wetting temperature, nanochannel size, and nanochannel surface properties on the flow behaviors of polyethylene melts in nanochannels are investigated in the following sections.

3.2. Flow behaviors of polymer melts in nanochannels under different wetting temperature

For the investigation of influence of wetting temperature on nanoflow of polymer melts, the nanochannels with a diameter of 80 nm and a length of about 50 μm was employed and the wetting time was set as 60 min. The dependence of displacements l_t of polymer melts into nanochannels on wetting temperature is shown in Fig. 4 and the according DSC melting curve of polyethylene is also presented.

The results indicate that the wetting temperature plays an important role on the displacement of polyethylene melts into nanochannels. The infiltration displacement is remarkably increasing with the increase of temperature from the T_m

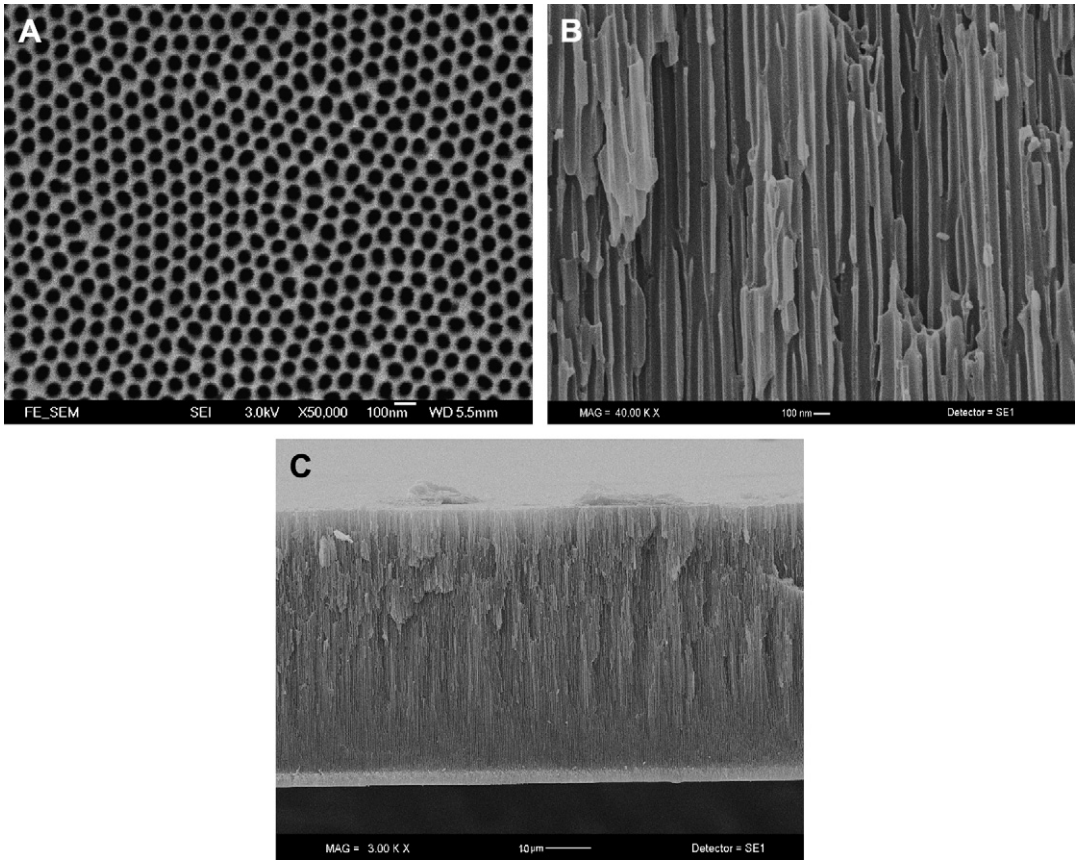

Fig. 2. SEM images of nanoporous alumina template and its nanochannels (A) top-view of template, (B) cross-section of nanochannels, and (C) cross-section of the whole nanochannels.

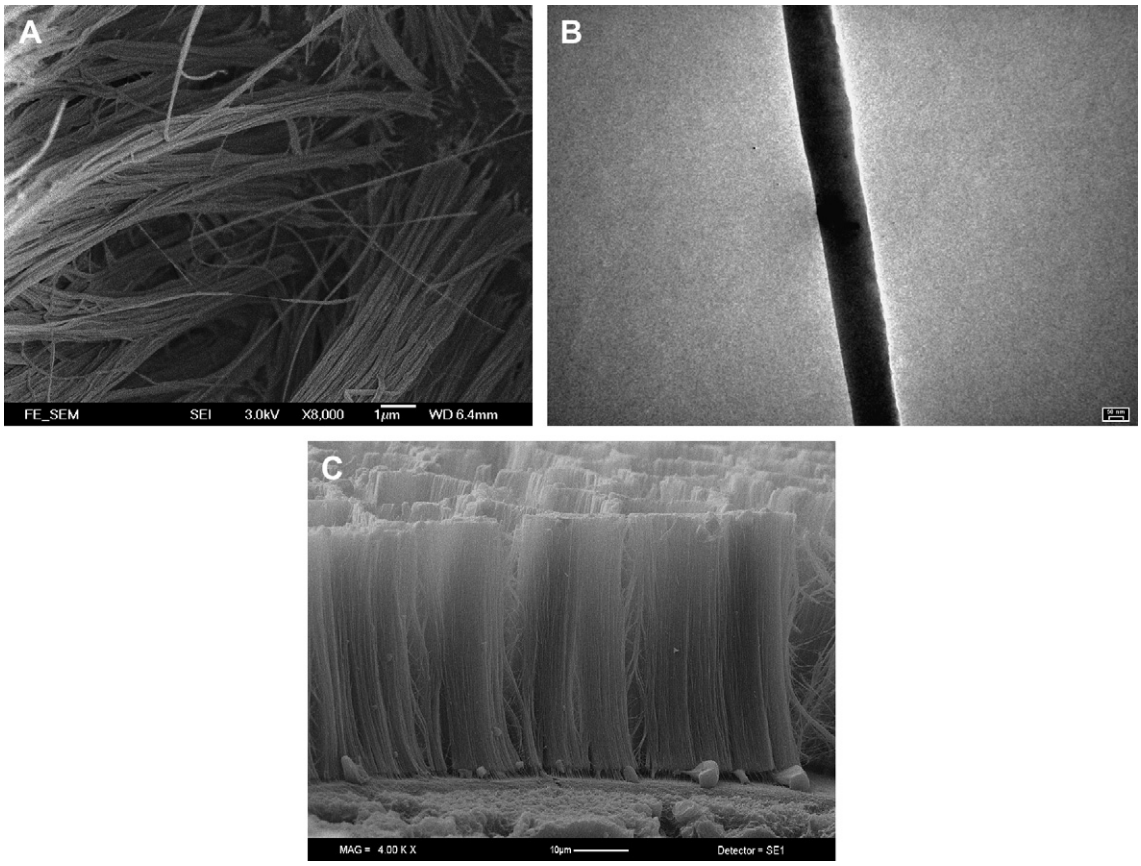

Fig. 3. SEM and TEM images of polyethylene nanofibers, (A) SEM image of nanofibers, (B) TEM image of a single nanofiber, and (C) SEM cross-section image of nanofibers on the substrate.

(129 °C) to the podium temperature of 160 °C on DSC thermograph. It indicates that the polymer melts can wet the alumina nanopores' inner walls with high-energy surface when most of lamellae of this semi-crystalline polymer are melted under the temperature far above the T_m [49,50]. Considering that the aspect ratio of nanofibers is equal to ~500 within the short wetting time of 60 min, so the flow rate of polyethylene melts in nanochannel can be considered very high when the wetting temperature is 160 °C.

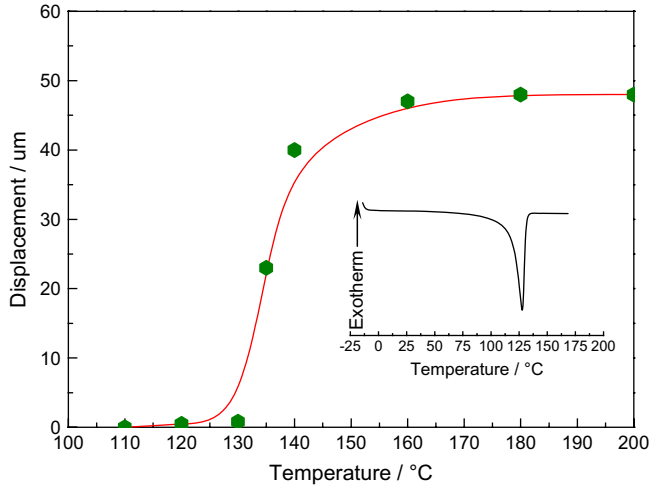

Fig. 4. The relationship between the displacements of polyethylene melts in nanochannels and the wetting temperature within the same wetting time.

The influence of wetting temperature on nanoflow of polymer melts in nanochannels can be ascribed to the wetting transition of melts on high-energy surface. For the wetting of solid substrates by liquids, a temperature T_w is predicted for a wetting transition from partial to complete regime, where T_w is called the wetting transition temperature [51]. When the wetting temperature is 160 °C, the polyethylene melts with low viscosity will be wetting the inner walls of nanochannels in a complete wetting regime. It should be pointed out that the displacement of melt is only determined in the scale less than 50 μm due to the limitation of maximum length of nanochannels. The higher flow displacement perhaps can be achieved at wetting temperature higher than 160 °C because the viscosity of melts is decreasing with the increase of temperature.

3.3. Flow behaviors of polymer melts in nanochannels with different sizes

At the wetting temperature of 160 °C, the nanoflow behavior of polyethylene melts in nanochannels with different diameters was studied. The relationship between displacements l_t of polymer melts into nanochannels and wetting time is shown in Fig. 5.

For three types of nanochannels with different diameters, the infiltration displacements of melts reach the maximum

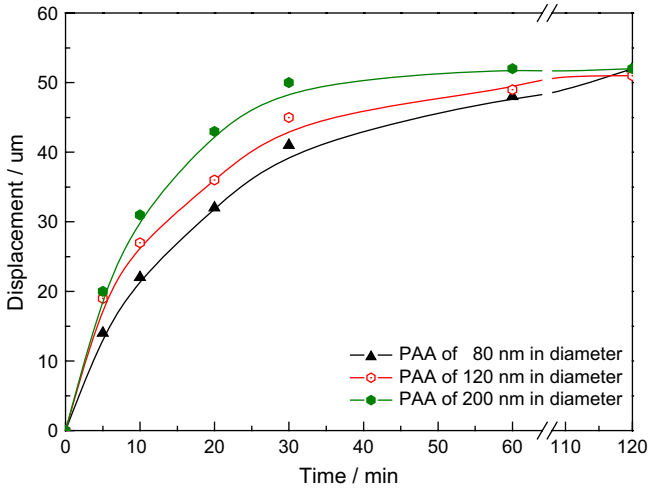

Fig. 5. The relationship between the displacements of polyethylene melts in nanochannels with different diameters and wetting time at the wetting temperature of 160 °C.

length of nanochannels (50 μm) only within 60 min. This demonstrates that the wetting of polyethylene melts in nanochannel is a rapid process as mentioned above. Furthermore, the flow rate is increasing with the increase of diameter of nanochannels. It suggests that the polymer melts are easier to be wetting into the nanochannels with larger size in the range of 80–220 nm. The dependence of infiltration displacements of polymer melts into nanochannels on wetting time is in accordance with the following Luacs–Washburn equation [52], which describes the relationship between capillary velocity of simple liquid into micro-/nano-channels and surface tension, contact angle, viscosity of liquid and the diameter of channels:

$$dz/dt = R\gamma \cos \theta_c/(4\eta z)$$

where z is the length of the melt column in the pore, t is the time, η is the viscosity of the melt, R is the hydraulic radius, γ is surface tension, and θ is contact angle. The presented results indicate that the flow rate of polymer melts into nanochannels on wetting time is dependent on the diameter of nanochannels and the polymer melts are easier to be wetting into the nanochannels with larger size in the range of 80–220 nm.

3.4. Flow behaviors of polymer melts in nanochannels with different surface properties

The alkylsilane self-assembled monolayers (SAMs) possessing a significantly low surface energy were often used on alumina surface to adjust their wettability property [53–56]. After the hydrolysis, condensation and curing at high temperature of octadecyltrimethoxysilane [40,54,57], the self-assembled monolayers on inner walls of nanochannels in PAA template are formed as illustrated in Fig. 6. The according infiltration displacements l_t of polyethylene melts in native nanochannels and SAMs treated nanochannels at the same wetting temperature are presented in Fig. 7.

From Fig. 7, it can be seen that the infiltration displacements and rate of polymer melts into SAMs treated nanochannels are less and lower than those in the native alumina nanochannels at the same wetting temperature. It can be explained by the decrease of surface free energy on alumina surface treated by SAMs, which is low surface free energy material. This phenomenon is also found for the contact angle or surface free energy of *n*-hexadecane (non-polar, low molecular weight analogues of polyethylene) on octadecyltrimethoxysilane modified alumina surface or silicon wafer [53,58]. Based on our results of contact angle measurement, the static contact angle of *n*-hexadecane on the SAMs treated alumina surface (41°) is higher than that on the native alumina surface (3°). In another word, the modified alumina nanochannels actually possess a significantly low surface free energy after the formation of self-assembled monolayers. According to the Laplace equation (Eq. (1)), the wetting driven force p will be decreasing on the modified surface as the γ is decreasing and the θ is

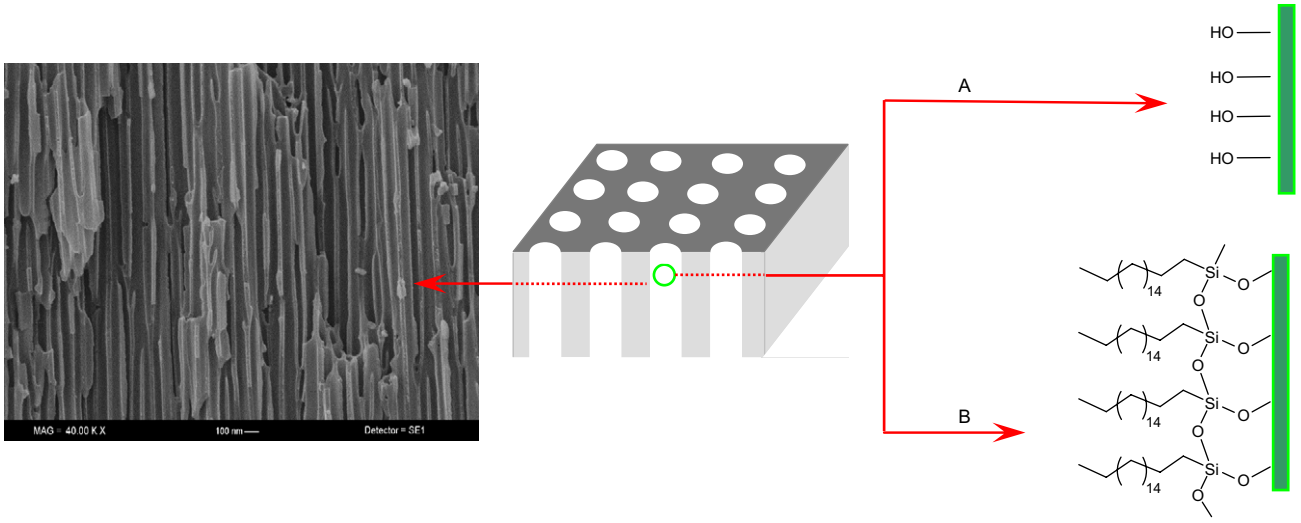

Fig. 6. The inner wall surface of PAA nanochannels, (A) native PAA template and (B) octadecyltrimethoxysilane self-assembled monolayers treated surface.

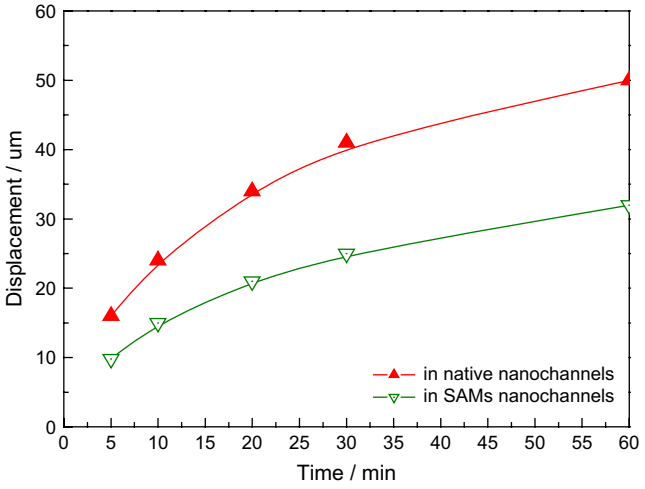

Fig. 7. The relationship between displacements of polyethylene melts in nanochannels with different inner walls surface properties at the wetting temperature of 160 °C.

increasing. So slow flow of polymer melts in nanochannels with SAMs treated alumina surface is observed at the wetting stage. Thus, as the presented results in Fig. 7, it reveals that the high surface free energy and solid–liquid interaction between melts and surface lead to noticeable flow of polymer melts in nanochannels at the wetting stage.

Integrated with the results mentioned in the above sections, it can be demonstrated that the flow rate of polymer melts into nanochannels at the wetting stage is mainly dependent on the wetting temperature, the size of nanochannels and surface properties of nanochannels. The wetting of polyethylene melts in nanochannels is a rapid process due to the high surface free energy of alumina nanochannels and wetting driven force. Considering the potential application of nanopores wetting nanotechnology, these results will be useful for the preparation of polymer-based nanomaterials and nano-devices using lithography, nano-injection and nano-extrusion strategies.

4. Conclusions

In conclusion, the polyethylene nanofibers with high aspect ratio are formed after the infiltration of their melts into the alumina nanochannels by nanopores wetting strategy. The wetting of polyethylene melts in nanochannels is a rapid process due to the high surface free energy of alumina nanochannels and wetting driven force. The polymer melts can wet and flow in nanochannels rapidly under the temperature much higher than the melting temperature. And the flow rate is increasing with the increase of diameter of nanochannels in the range of 80–220 nm. The displacement and rate of polymer melts into nanochannels treated by octadecyltrimethoxysilane self-assembled monolayers with low surface free energy are lower than that in the pure alumina nanochannels with high surface free energy at the same wetting temperature. The high surface energy and solid–liquid interaction between melts and surface lead to more noticeable flow of polymer melts in nanochannels at the wetting stage.

Acknowledgment

This work was supported by the Hong Kong Research Grants Council (PolyU5314/05E) and postdoctoral fellow grant project of the Hong Kong Polytechnic University.

References

[1] Craighead HG. Science 2000;290:1532–5.
[2] Sun Y, Kwok YC. Anal Chim Acta 2006;556:80–96.
[3] Ahn CH, Choi JW, Beaucage G, Nevin JH, Lee JB, Puntambekar A, et al. Proc IEE 2004;92:254–73.
[4] Ramakrishna S, Lala NL, Garudadhwaj H, Ramaseshan R, Ganesh VK. Top Appl Phys 2007;109:377–92.
[5] Sokuler M, Gheber LA. Nano Lett 2006;6:848–53.
[6] Chronis N, Lee LP. Lab on a Chip 2004;4:125–30.
[7] Conrad PG, Nishimura PT, Aherne D, Schwartz BJ, Wu DM, Fang N, et al. Adv Mater 2003;15:1541–4.
[8] Vogler M, Wiedenberg S, Muhlberger M, Bergmair I, Glinsner T, Schmidt H, et al. Microelectron Eng 2007;84:984–8.
[9] Mata A, Fleischman AJ, Roy S. J Micromech Microeng 2006;16:276–84.
[10] Wang XF, Um IC, Fang DF, Okamoto A, Hsiao BS, Chu B. Polymer 2005;46:4853–67.
[11] Zuwei MAZ, Kotaki M, Yong T, He W, Ramakrishna S. Biomaterials 2005;26:2527–36.
[12] Kim Y, Choi Y, Kim YJ, Kang S. Jpn J Appl Phys Part 1 Regular Pap Short Notes Rev Pap 2005;44(5B):3591–5.
[13] Ueda M, Takamura Y, Horiike Y, Baba Y. Jpn J Appl Phys Part 1 Regular Pap Short Notes Rev Pap 2004;43(7A):4417–8.
[14] Li HY, Ke YC, Hu YL. J Appl Polym Sci 2006;99:1018–23.
[15] Helmy R, Kazakevich Y, Ni CY, Fadeev AY. J Am Chem Soc 2005;127:12446–7.
[16] Galea TM, Attard P. Langmuir 2004;20:3477–82.
[17] Bonaccurso E, Butt HJ, Craig VSJ. Phys Rev Lett 2003;90:144501.
[18] Jabbarzadeh A, Atkinson JD, Tanner RI. Phys Rev E 2000;61:690–9.
[19] Sbragaglia M, Benzi R, Biferale L, Succi S, Toschi F. Phys Rev Lett 2006;97:204503.
[20] He YD, Qian HJ, Lu ZY, Li ZS. Polymer 2007;48:3601–6.
[21] Yung KL, He L, Xu Y, Shen YW. Polymer 2005;46:11881–8.
[22] Yung KL, He L, Xu Y, Shen YW. Polymer 2006;47:4454–60.
[23] Yung KL, He L, Xu Y, Shen YW. J Chem Phys 2005;123:246101.
[24] Muller M, MacDowell LG. J Phys Condens Matter 2003;15:R609–53.
[25] Pit R, Hervet H, Leger L. Phys Rev Lett 2000;85:980.
[26] Joseph P, Tabeling P. Phys Rev E 2005;71:035303.
[27] Cottin-Bizonne C, Jurine S, Baudry J, Crassous J, Restagno F, Charlaix E. Eur Phys J E 2002;9:47–53.
[28] Alvine KJ, Shpyrko OG, Pershan PS, Shin K, Russell TP. Phys Rev Lett 2006;97:175503.
[29] Sinha S, Rossi MP, Mattia D, Gogotsi Y, Baua HH. Phys Fluids 2007;19:013603.
[30] Cheng JT, Giordano N. Phys Rev E 2002;65:031206.
[31] Xu H, Shirvanyants D, Beers K, Matyjaszewski K, Rubinstein M, Sheiko SS. Phys Rev Lett 2004;3:206103.
[32] Saritha S, Neogi P, Wang JC. Polymer 2006;47:6263–6.
[33] Steinhart M, Wehrspohn RB, Gösele U, Wendorff JH. Angew Chem Int Ed 2004;43:1334–44.
[34] Steinhart M, Zimmermann S, Golring P, Schaper AK, Gösele U, Weder C, et al. Nano Lett 2005;5:429–34.
[35] Zheng RK, Yang Y, Wang Y, Wang J, Chan HLW, Choy CL, et al. Chem Commun 2005:1447–9.
[36] Steinhart M, Senz S, Wehrspohn RB, Gösele U, Wendorff JH. Macromolecules 2003;36:3646–51.
[37] Pisula W, Kastler M, Wasserfallen D, Davies RJ, García-Gutiérrez M, Müllen K. J Am Chem Soc 2006;128:14424–5.

[38] Steinhart M, Wendorff JH, Greiner A, Wehrspohn RB, Nielsch K, Schilling J, et al. Science 2002;296:1997.
[39] Kim E, Xia YN, Whitesides GM. J Am Chem Soc 1996;118:5722–31.
[40] Jayaraman K, Okamoto K, Son SJ, Luckett C, Gopalani AH, Lee SB, et al. J Am Chem Soc 2005;127:17385–92.
[41] Okamoto K, Shook CJ, Bivona L, Lee SB, English DS. Nano Lett 2004; 4:233–9.
[42] Son Y. Polymer 2007;48:632–7.
[43] Jeszka JK, Pakula T. Polymer 2006;47:7289–301.
[44] Somani RH, Yang L, Zhu L, Hsiao BS. Polymer 2005;46:8587–623.
[45] Masuda H, Fukuda K. Science 1995;268:1466–8.
[46] Xu TT, Piner RD, Ruoff RS. Langmuir 2003;19:1443–5.
[47] Moon SI, McCarthy TJ. Macromolecules 2003;36:4253–5.
[48] Zhang MF, Dobriyal P, Chen JT, Russell TP. Nano Lett 2006;6:1075–9.
[49] Kong J, Fan XD, Jia M. J Appl Polym Sci 2004;93:2542–9.
[50] Kong J, Fan XD, Qiao WQ, Xie YC, Si QF, Tang YS. Polymer 2005;46: 7644–51.
[51] Cahn JW. J Chem Phys 1977;66:3667–72.
[52] Martic G, Gentner F, Seveno D, Coulon D, De Coninck J, Blake TD. Langmuir 2002;18:7971–6.
[53] Morita M, Koga T, Hideyuki Otsuka, Atsushi Takahara. Langmuir 2005; 21:911–8.
[54] Carino SR, Tostmann H, Underhill RS, Logan J, Weerasekera G, Culp J, et al. J Am Chem Soc 2001;123:767–8.
[55] Sagiv J. J Am Chem Soc 1980;102:92–8.
[56] Laibinis PE, Whitesides GM. J Am Chem Soc 1992;114:1990–5.
[57] Fontaine P, Goldmann M, Rondelez F. Langmuir 1999;15:1348–52.
[58] Schmatko T, Hervet H, Leger L. Phys Rev Lett 2005;94:244501.